HAL
open science

Thermodynamic Optimization of Electrical and Thermal Energy Production of PV Panels and Potential for Valorization of the PV Low-Grade Thermal Energy into Cold

Anis Idir, Maxime Perier-Muzet, David Aymé-Perrot, Driss Stitou

To cite this version:

Anis Idir, Maxime Perier-Muzet, David Aymé-Perrot, Driss Stitou. Thermodynamic Optimization of Electrical and Thermal Energy Production of PV Panels and Potential for Valorization of the PV Low-Grade Thermal Energy into Cold. Energies, 2022, 15 (2), pp.498. 10.3390/en15020498 . hal-03522319

HAL Id: hal-03522319

https://hal.science/hal-03522319v1

Submitted on 12 Jan 2022

HAL is a multi-disciplinary open access archive for the deposit and dissemination of scientific research documents, whether they are published or not. The documents may come from teaching and research institutions in France or abroad, or from public or private research centers.

L'archive ouverte pluridisciplinaire **HAL**, est destinée au dépôt et à la diffusion de documents scientifiques de niveau recherche, publiés ou non, émanant des établissements d'enseignement et de recherche français ou étrangers, des laboratoires publics ou privés.

energies

MDPI

Article

Thermodynamic Optimization of Electrical and Thermal Energy Production of PV Panels and Potential for Valorization of the PV Low-Grade Thermal Energy into Cold

Anis Idir [1,2,3,*], Maxime Perier-Muzet [1,3], David Aymé-Perrot [2] and Driss Stitou [1]

[1] PROMES Laboratory (PROcess, Material and Solar Energy), CNRS-UPR8521, Rambla de la Thermodynamique, Tecnosud, 66100 Perpignan, France; maxime.perier-muzet@univ-perp.fr (M.P.-M.); driss.stitou@promes.cnrs.fr (D.S.)

[2] TotalEnergies SE, 2 Place Jean Millier–, 92078 Courbevoie, France; david.aymeperrot@totalenergies.com

[3] Department of Engineering Science, Faculty of Exact Sciences, University of Perpignan Via Domitia, 52 Avenue Paul Alduy, 66100 Perpignan, France

* Correspondence: anis.idir@promes.cnrs.fr; Tel.: +33-767-256-898

Abstract: In the present study, the evaluation of potential improvement of the overall efficiency of a common PV panel, valorizing the heat extracted by a heat exchanger that is integrated on its back side, either into work using an endoreversible Carnot engine or into cold by using an endoreversible tri-thermal machine consisting of a heat-driven refrigeration machine operating between three temperature sources and sink (such as a liquid/gas absorption machine), was carried out. A simplified thermodynamic analysis of the PV/thermal collector shows that there are two optimal operating temperatures $\widetilde{T}_h$ and T_h^* of the panels, which maximize either the thermal exergy or the overall exergy of the PV panel, respectively. The cold produced by the endoreversible tri-thermal machine during the operating conditions of the PV/thermal collector at $\widetilde{T}_h$ is higher with a coefficient of performance (COP) of 0.24 thanks to the higher heat recovery potential. In the case of using the cold produced by a tri-thermal machine to actively cool of an additional PV panel in order to increase its electrical performances, the operating conditions at the optimal temperature T_h^* provide a larger and more stable gain: the gain is about 12.2% compared with the conventional PV panel when the operating temperature of the second cooled panel varies from 15 to 35 °C.

Keywords: power and cold cogeneration; energy performance; exergy analysis; solar energy

check for updates

Citation: Idir, A.; Perier-Muzet, M.; Aymé-Perrot, D.; Stitou, D. Thermodynamic Optimization of Electrical and Thermal Energy Production of PV Panels and Potential for Valorization of the PV Low-Grade Thermal Energy into Cold. *Energies* **2022**, *15*, 498. https://doi.org/10.3390/en15020498

Academic Editor: Philippe Leclère

Received: 16 November 2021
Accepted: 6 January 2022
Published: 11 January 2022

Publisher's Note: MDPI stays neutral with regard to jurisdictional claims in published maps and institutional affiliations.

Copyright: © 2022 by the authors. Licensee MDPI, Basel, Switzerland. This article is an open access article distributed under the terms and conditions of the Creative Commons Attribution (CC BY) license (https://creativecommons.org/licenses/by/4.0/).

1. Introduction

Photovoltaic (PV) technology is currently one of the most widely used technologies for producing renewable electricity with 20.6% of the 6523 TWh renewable electricity generation worldwide in 2018 [1]. During the period 2009–2019, photovoltaic technology was the fastest increasing renewable energy technology, with an average cumulative increase of 36% of grid-connected installation [1].

The conversion of solar radiation directly into electricity with the highest possible efficiency is a research topic of great interest in the scientific community. The PV conversion for a simple Si-based p-n junction is, however, limited by the theoretical Shokley–Queiser limit: only a maximum of 31% of the non-concentrated solar radiation can be converted into electricity [2]. As shown in Figure 1 and proposed by Li et al. [3], representing the energy balance of PV conversion under 1.5 AM solar spectrum, about 67.6% of the incoming radiative energy is converted into heat by crystalline Si PV panels, which correspond to 50.2% to the thermalization of excess energy of photons with energy above the Eg band gap and 17.4% of the thermal absorption of photons below the bandgap. The produced heat increases the temperature of the cells, which in turn reduces the ability of the PV panel to generate electricity. In order to simplify the comparison of the performance of PV

panels, electrical efficiencies are generally measured under standard test conditions (STC) where the panel temperature is 25 °C. The widely used relationship between temperature and efficiency of mono-crystalline silicon PV cells indicates that electricity production decreases by approximately 0.004–0.005 K^{-1}, also defined as the temperature coefficient [4,5]. In addition to the degradation of PV panel performance with temperature, the life cycle analysis of PV panels led by Nehme and al. [6] shows that the temperature is also one of the most impacting parameters that affects the degradation rate of PV panel lifetime. Ogbomo et al. investigated the impact of PV cell temperature on solder joint interconnection degradation for a crystalline silicon PV module in a hot climate. The prediction model developed by the authors forecasted that the PV module lifetime, due to the failure of specific parts such as joints between the cells, is 18.5 years in London and 9 years in a warm climate, respectively. The module lifetime in London is close to the 25-year warranty. The 9 years predicted in the warm climate gives an indication of the high failure rate observed in hot and harsh regions [7]. Reducing the operating temperature is thus a key solution to increase the lifetime of PV panels and minimize their performance degradation.

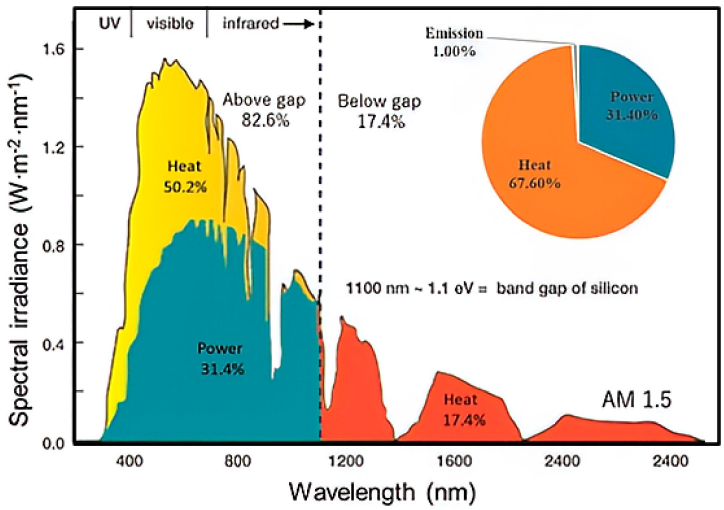

Figure 1. Energy balance of the PV conversion by crystalline Si cell according to Li et al. [3].

To improve the electrical production of PV cells, two fundamental routes are investigated in the literature. The first way focuses on the development of new, more efficient PV material, seeking to reduce energy losses due to the spectral mismatch. For that, many associations of different PV materials are notably studied and developed (e.g., tandem cells) to valorize a higher part of the solar spectrum and to increase the solar conversion. The second field of research is focused on the temperature control of solar cells. Research on cooling technology of PV panels is currently receiving increased attention in order to improve the performance of PV panels. Many cooling methods can be found in the literature and in most cases the thermal energy is wasted [8–11]. However, regarding existing technologies for the thermal management of PV panel, it seems that few of them are able to both collect and valorize the thermal energy produced from PV. This paper focuses on heat recovery and the way to valorize this heat. This seems to be a promising way to increase the overall efficiency of PV panels. The thermal energy of the PV panel can be used to satisfy a need in heat but also to drive thermodynamic processes in order to transform it into additional electricity or cold.

The thermal energy generated by a photovoltaic panel can be used to be converted directly into electricity. The use of a thermoelectric generator (TEG) module that converts heat to electricity through the Seebeck effect was studied by Bjork et al. to evaluate the maximum theoretical performance of coupling a non-concentrated PV panel and a TEG. Considering the TEG material characteristics, its associated Carnot efficiency, and a Shokley–Queisser limit of 33% for an idealized single p-n junction cell with a band gap

value of 1.34 eV, while it is around 31% for c-Si based on a band gap of 1.12 eV, these authors also showed that the theoretical electrical conversion efficiency can be increased to 37.5% [12]. Another direct heat-to-electricity conversion has been studied by Fathabadi et al.: the thermally regenerative electrochemical cycle (TREC), which is based on the thermogalvanic effect and the temperature dependence of the electrode potential. This cycle is realized by charging and discharging an electrochemical cell [13]. During the charging (heating process), a difference between the voltages of the two charged electrodes is created, allowing for the production of electrical energy during the discharge process of the TREC cell. These authors compared the electricity production by TEG and TREC devices placed behind PV modules. They found that the use of TREC devices compensates for about 85% of the PV power reduction compared to STC conditions due to temperature increase, while only 23% is compensated when a TEG module is used [13].

Solar PV-Thermal panels (PVT), unlike conventional photovoltaic systems, are specifically designed to produce both electricity and heat. Depending on the architecture of these PVTs and the operating parameters, the electrical production and/or heat production can be optimized according to the desired application, leading to a higher overall energy efficiency than conventional photovoltaic panels [14,15]. The electrical output or thermal output of a PVT panel can be improved at the expense of the other according to the intended application and depends on the choice of parameters: PVT technology (glazed or unglazed), the nature and mass flow rate of the heat transfer fluid, PV cell material impacting the PV efficiency, packing factors, solar irradiation, wind speed, and ambient temperature. Generally, the thermal energy generated by the PVT panel is used to satisfy a heating demand such as the heating of a building by a working fluid (water or air). Chow et al. compared the performance of glazed and unglazed water PVT panels experimentally and numerically. The glazed water PVT reached a higher energy yield and outlet temperature than the unglazed one because of its higher thermal energy efficiency. However, the exergy yield is more important for the unglazed PVT than the glazed one because of the higher electrical energy yield [14]. Many authors also studied a combined PVT-PCM system that is actively cooled by a heat transfer fluid (water or nanofluid). Sarafraz et al. experimentally investigated and carried out an efficiency comparison of a standalone PV, PV-PCM, water-cooled PVT-PCM, and nanofluid-cooled PVT-PCM. The best performance is reached in the nanofluid-cooled PVT-PCM system because of the thermal ability of the heat transfer fluid to efficiently cool the PV panel, which in return increases the electricity production [16].

Currently, PVT-driven heat pump technology is gaining more and more popularity in the research field for building applications [17–20]. Such a combination allows for a tri-generation system that can produce electricity, heat, and cold at the same time. The PVT collector unit can be used to feed the evaporator of the heat pump for heating purposes, with an amplified effect. On the other hand, the heat pump can be also used to provide a cooling effect for air-conditioning purposes. Zhou et al. [17] evaluated the potential and the performance of such a tri-generation PVT-driven heat pump system operating under natural weather conditions. The experimental study they carried out showed that the electrical efficiency, the heating coefficient of performance (COP), and the cooling COP achieved were 8.7%, 5.3, and 2.3, respectively.

To more precisely analyze the performance of these systems that can produce several useful effects (electricity, heat, or cold), different performance criteria can be used:

- Energy-based criteria such as electrical efficiency that only takes into account the electricity produced, thermal efficiency that only takes into account the heat production, or the overall efficiency that considers the sum of the energies of all the useful effects produced.
- Exergy-based criteria such as exergy efficiency that takes into account the exergy associated to all the useful effects produced.

Nevertheless, an overall energy yield based upon two different forms of energy (heat and electricity) is generally not very representative of the real potential of the global energy because of the difference in the energy quality between electricity and thermal energy.

In order to evaluate the potential of the overall energy yield of PVT panels, different approaches are used in the literature to assess and qualify the potential of energy with different forms. The first one is based on the primary energy consumption to produce the different forms of energy. In particular, the primary energy (PE) required to produce a given amount of electrical energy is assumed to follow the ratio of about 2.63 kWh_{PE}/kWh_{el} [21,22], which corresponds to the efficiency of a conventional power plant of 38%. The second method is based on a thermodynamic analysis using the first and second laws, in which the overall energy produced by the PVT panel is characterized throughout its exergy content. The exergy content of energy is defined as the maximum work that can be obtained directly from this energy (as for electricity), or by using a Carnot machine, ideally converting this energy (thermal energy) into work [14,23,24].

To sum up, the literature shows that there are several possible ways to use and valorize the thermal energy generated by PV collectors to increase the overall energy or exergy efficiency. Many parameters influence the performance of PVT collectors in term of electricity and/or thermal energy production. Such a system has to be properly chosen according to the targeted utilization of the energies to be produced and the criteria to be met. In this work, a theoretical study of a novel combination is carried out: a PV system is coupled with a thermal collector. Such a coupled PV/thermal collector system (PV/TC) can then be used to thermally feed a di-thermal or a tri-thermal machine for valorizing the thermal energy. The basic idea of such an association is to improve, on the one hand, the electrical performance of the PV panels by limiting their temperature rise, and on the other hand, to valorize the heat collected on the PV panels into additional work by a di-thermal machine or into cold by a tri-thermal machine, thus increasing the overall energetic and exergetic yield. The cold produced can also be used to cover the cooling needs in buildings or to allow for an active cooling of the PV panels, which furthers the production of electricity. The recovery of the heat generated by the PV panel and its valorization to produce a cooling effect by the tri-thermal machine, which allows the panels to operate at a temperature lower than or at least close to the ambient temperature and improves the electrical efficiency of the PV panels. These operating conditions are original in comparison with the usual systems studied in literature. The objective of this study is to evaluate the theoretical performances that could be achieved by such a novel combination.

2. Materials and Method: Thermodynamic Assessment Methodology

The methodology that is presented here for the thermodynamic evaluation of the potential of valorization of the heat generated in a PV panel requires to define in first step the different energy flows between the system and its environment. In a second step, different types of coupling between the PV/TC collector and thermally driven processes are presented according to different targeted applications: heat valorization into additional work production that can be further converted into electricity, or converted into cold, which can be used either for the thermal comfort of buildings or for the cooling of an additional PV panel in order to increase overall electrical performances.

2.1. Energy and Exergy Analysis of a PV/Thermal Collector System

In conventional PVT panels, a heat exchanger is usually integrated on the back surface to absorb the heat produced by the PV panel and transfer it to a coolant fluid, which is generally water or air. Such a thermal collector integration approach can be easily implemented into an already installed PV panel without major modification, giving rise to a PV/TC system. In this way, the extraction of heat from the PV panel will limit the temperature increase of the panel and could ideally decrease its temperature close to the ambient one, allowing, in this case, for a maximum recovery of the generated heat. This reduction of the PV operating temperature allows us to considerably improve the electrical production and to get closer to the performances obtained under standard test conditions (STC @ 25 °C/1000 W/m^2). However, for these operating conditions, the extracted heat cannot be exploited due to its too low temperature level and exergy content. The latter

must be produced at a higher temperature to be exploitable and valorized. At the same time, due to the degradation of the electrical performance with increasing temperature, the operating temperature should be optimized to reach optimal global performances. Another point to consider is that as the operating temperature of the PV panel increases, the amount of heat that can be extracted decreases and becomes zero for the stagnation temperature (T_{st}) for which the panel is in thermal equilibrium with the ambient environment. The thermal behavior of the PV panel thus has to be carried out from an energetic point of view to assess the amount of energy involved, as well as from an exergetic point of view to evaluate the theoretical potential to exploit the extracted thermal energy.

2.1.1. Energetic Analysis of a PV/Thermal Collector System

The different types of energy flows that are involved in a PV/thermal collector (PV/TC) system, according to the operating conditions applied to the panel in Figure 2, are considered.

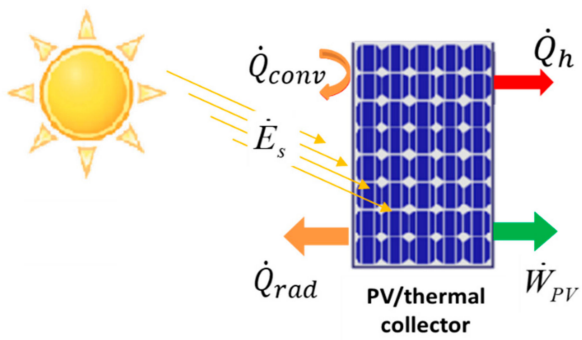

Figure 2. Schematic representation of the flows exchanged between a PV/thermal collector panel and its surrounding with the following: $\dot{E}_s$ is the absorbed solar incoming irradiation, $\dot{Q}_h$ is the useful thermal energy, $\dot{W}_{PV}$ is the produced electrical power, $\dot{Q}_{conv}$ is the natural and forced convective heat losses, and $\dot{Q}_{rad}$ are the radiative heat losses.

Assuming that the PV/TC panel temperature is homogeneous, and the back and lateral and side surfaces of the panel are adiabatic, only the exchanges of the front surface with the external environment are considered (convective with the ambient and radiative with the sky). Applying the first law of the thermodynamics on PV/TC association, which is considered as a single uniform control volume and in steady-state operation, gives the following:

$$\dot{E}_s - \dot{Q}_{conv} - \dot{Q}_{rad} - \dot{W}_{PV} - \dot{Q}_h = 0 \quad (1)$$

where $\dot{E}_s$ is the absorbed solar incoming irradiation, $\dot{W}_{PV}$ is the electrical power production, $\dot{Q}_h$ is the thermal power production, and $\dot{Q}_{conv}$, $\dot{Q}_{rad}$ are the convective and radiative heat losses, respectively.

The total solar energy that is absorbed by the PV panel is as follows:

$$\dot{E}_s = (\alpha\tau) I_G \quad (2)$$

where α is the solar absorptance of PV layers, τ is the solar transmittance of the glazing, and I_G is the global incident irradiation.

The electricity energy produced by the cell is expressed by Equation (3) [25]:

$$\dot{W}_{PV} = (\alpha\tau) I_G \eta_{PV} = (\alpha\tau) I_G \eta_{ref} \left[1 - \beta_{ref}(T_{cell} - T_{STC})\right] \quad (3)$$

In which η_{PV} is the electrical efficiency depending on the actual operating cell temperature and η_{ref} is the reference electrical efficiency of the PV module operating at the standard test conditions (STC) T_{STC} = 25 °C under a global solar irradiation I_G = 1000 W·m^{-2} [25]. The temperature coefficient β_{ref} is based on the material properties, and T_{cell} is the oper-

ating cell temperature. The values of η_{ref} and β_{ref} used for this study are from standard commercial PV panels.

To determine the heat exchange between the panel and the ambient air, a coefficient of global convective (natural and forced) heat transfer is considered. Test et al. experimentally evaluated the convective exchange coefficient of a plate placed in the natural environment and the wind speed at a height of 1 m above the plate was recorded. They were able to develop a linear correlation that is used here [26]:

$$\dot{Q}_{conv} = h_{conv}(T_{cell} - T_{amb}) \tag{4}$$

The convective heat coefficient transfers h_{conv} depends on the wind velocity V_w as follows:

$$h_{conv} = 2.56V_w + 8.55$$

The rate of radiative heat exchange is given by the Stephan-Boltzman law [27]:

$$\dot{Q}_{rad} = \sigma\varepsilon\left(T_{cell}^4 - T_{sky}^4\right) \tag{5}$$

where ε is the emissivity of the PV panel and σ is the Stephan–Boltzmann constant. The temperature of the sky T_{sky} depends on the ambient temperature T_{amb} and is expressed as follows: $T_{sky} = 0.0552T_{amb}^{1.5}$.

The energy analysis can be carried by considering the following performance criteria:

- Electrical efficiency:

$$\eta_{PV} = \frac{\dot{W}_{PV}}{\dot{E}_s} \tag{6}$$

- Thermal efficiency:

$$\eta_{th} = \frac{\dot{Q}_h}{\dot{E}_s} \tag{7}$$

- Overall efficiency:

$$\eta_{gl} = \eta_{PV} + \eta_{th} \tag{8}$$

2.1.2. Exergetic Analysis of the PV/Thermal Collector System

The exergy analysis allows us to evaluate the quality of energy involved in a system and to standardize the evaluation of the thermodynamic quality of systems in which different forms of energy are involved. The exergy quantifies the maximum work that can be ideally produced by an ideal reversible process, such as a Carnot engine, and can thus be defined as the work content of the energy. The electrical energy is a high-quality energy and is thus considered as pure exergy as it can be ideally fully converted into work using an ideal electrical motor. The thermal exergy (characterizing the quality of the thermal energy) depends on its temperature (T_h) relative to the reference temperature (T_0), for which the exergy content of the thermal energy is zero (dead state). The thermal exergy corresponds to the maximum amount of work that can be ideally produced by a Carnot cycle consuming the heat $\dot{Q}_h$ at T_h and releasing heat at T_0:

$$Ex = \dot{Q}_h\left(1 - \frac{T_0}{T_h}\right) = \dot{Q}_h.\theta_h$$

The Carnot factor $\theta_h = 1 - \frac{T_0}{T_h}$ is introduced to estimate the exergy content of a given amount of thermal energy available at a temperature T_h. In that study, the reference temperature T_0 is equal to T_{amb}.

To evaluate the transformable equivalent work and estimate the exergy destroyed in the PV/TC panel, and hence its thermodynamic quality, an exergy balance of the system can also be expressed as:

$$\dot{E}x_s - \dot{W}_{PV} - \dot{E}x_{\dot{Q}_h} - (\dot{E}x_{\dot{Q}_{conv}} + \dot{E}x_{\dot{Q}_{rad}}) - \dot{E}x_{des} = 0 \tag{9}$$

Several methods are proposed in the literature [28] to determine the solar exergy Ex_s of the incoming irradiation. One of the most commonly used calculation methods is proposed by Chow [14] considering a temperature T_s of the sun of 6000 K:

$$\dot{E}x_s = \dot{E}_s\left(1 - \frac{T_{amb}}{T_s}\right) \tag{10}$$

Additionally, the exergy of heat $\dot{E}x_{\dot{Q}_h}$ recovered at the operating temperature T_{cell} of the panel is expressed as follows:

$$\dot{E}x_{\dot{Q}_h} = \dot{Q}_h\left(1 - \frac{T_{amb}}{T_{cell}}\right) \tag{11}$$

Since electrical energy can be ideally converted entirely into work, by definition, the exergy of the electricity production is the electrical energy rate $\dot{W}_{PV}$.

From these definitions, the electrical exergy efficiency, thermal exergy efficiency, and overall exergy of a PV/TC system can be calculated from the following relations:

$$\eta_{ex_{PV}} = \frac{\dot{W}_{PV}}{\dot{E}x_s} \tag{12}$$

$$\eta_{ex_{th}} = \frac{\dot{E}x_{\dot{Q}_h}}{\dot{E}x_s} \tag{13}$$

$$\eta_{ex_{gl}} = \frac{\dot{W}_{PV} + \dot{E}x_{\dot{Q}_h}}{\dot{E}x_s} = \eta_{ex_{PV}} + \eta_{ex_{th}} \tag{14}$$

2.2. Thermally Driven Systems Coupled to the PV/Thermal Collector Panel for Heat Valorization

In this part, an analysis of different energy conversion systems coupled to a PV/TC system for the valorization of the produced heat is carried out. Indeed, the heat can be valorized in work by using a di-thermal engine cycle, or in cold by using a tri-thermal machine. Such a coupling will allow us to reduce the PV panel operating temperature, thus improving its electrical performances, and produce work or cold that will increase the overall performances of the system. The output energies of each coupling are analyzed and evaluated for each configuration to determine the optimal operating conditions according to the desired application.

2.2.1. PV/Thermal Collector System Coupled to a Di-Thermal Endoreversible Carnot Engine for Additional Work Production

The first combination consists in coupling the PV/TC system with a di-thermal machine exploiting the heat produced by the PV/TC, in order to produce a useful work that can be later converted in additional electricity, as depicted in Figure 3.

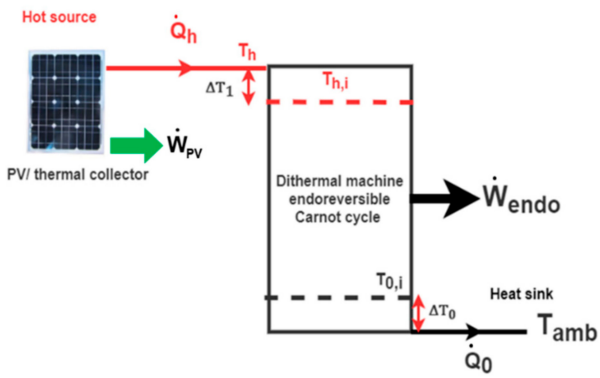

Figure 3. Coupling PV panel/thermal collector with an endoreversible Carnot engine cycle.

The considered di-thermal machine is an endoreversible Carnot engine [29]. This conceptual machine enables a more realistic analysis in comparison to the Carnot machine one. It takes into account the thermodynamic irreversibilities caused by the heat transferred between the cycle and the heat sources and sinks. The cycle then operates in a reversible way between internal temperatures ($T_{h,i}$) and ($T_{0,i}$), with no internal thermodynamic irreversibility. Therefore, the work $\dot{W}_{endo}$ that can be produced by the consumption of a given amount of thermal power $\dot{Q}_h$ at T_h can be estimated by considering the thermal pinches required for the heat exchange as:

$$\dot{W}_{endo} = \dot{Q}_h\left(1 - \frac{T_{0,i}}{T_{h,i}}\right) = \dot{Q}_h\left(1 - \frac{T_{amb} + \Delta T_0}{T_h - \Delta T_1}\right) \tag{15}$$

With a work engine efficiency cycle defined as follows [29]:

$$\eta_{endo} = \frac{\dot{W}_{endo}}{\dot{Q}_h} = 1 - \frac{T_{amb} + \Delta T_0}{T_h - \Delta T_1} \tag{16}$$

The temperature differences ΔT that are required for heat exchange between the external sources with the endoreversible Carnot engine are estimated under given realistic heat exchange coefficients by the following equations.

$$\dot{Q}_0 = (US)_0 \Delta T_0 \tag{17}$$

$$\dot{Q}_h = (US)_h \Delta T_1 \tag{18}$$

where $(US)_0$ and $(US)_h$ are the global heat conductance between the endoreversible Carnot engine with the ambient and the PV/TC, respectively.

2.2.2. PV/Thermal Collector System Coupled to a Tri-Thermal Machine for Cold Production

The second combination consists in coupling the PV/TC system with a tri-thermal machine in order to valorize the heat produced into cold as presented in Figure 4. A tri-thermal system is a closed thermodynamic system that exchanges only thermal energy with the external thermal sources/sinks. It operates between three different temperature levels: a hot source temperature noted T_h, a cold source temperature noted T_c, and a heat sink temperature T_{amb} that generally corresponds to the ambient environment. $\dot{Q}_h$ and $\dot{Q}_c$ are the heat quantities exchanged between the system and the external thermal sources at T_h and T_c, respectively.

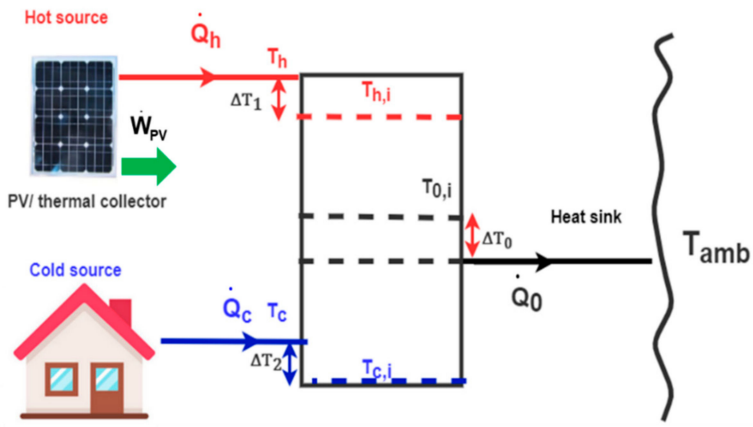

Figure 4. Schematic view of the coupling of a PV/TC system with a tri-thermal machine operating between three temperature levels for the production of usable cold in the building.

From a thermodynamic point of view, the tri-thermal system can be considered as the result of the coupling of two di-thermal cycles: an engine cycle and a reverse refrigeration cycle. Therefore, this tri-thermal system can be analyzed as an endoreversible machine consisting in the coupling of two endoreversible di-thermal cycles: an endoreversible engine cycle operating between T_h and T_{amb} coupled to an endoreversible refrigeration cycle operating between T_c and T_{amb}. The overall performance of the endoreversible tri-thermal machine can thus be realistically characterized by considering the thermodynamic irreversibilities due only to the external heat exchange as follows [30]:

$$COP_{endo}^{3T} = \eta_{endo} COP_{endo}^{2T} \tag{19}$$

With the endoreversible engine cycle efficiency η_{endo} defined by the Equation (16).

The produced work by the first cycle is internally consumed by the second reverse cycle to produce cold ($\dot{Q}_c$) at T_c, releasing heat ($\dot{Q}_0$) also at T_{amb}. This performance of this refrigeration cycle can also be characterized through its endoreversible coefficient of performance defined as:

$$COP_{endo}^{2T} = \frac{\dot{Q}_c}{\dot{W}_{endo}} = \frac{1}{\frac{T_{0,i}}{T_{c,i}} - 1} = \frac{T_c - \Delta T_2}{(T_{amb} + \Delta T_0) - (T_c - \Delta T_2)} \tag{20}$$

where the temperature differences ΔT_2 and ΔT_0 that are required for heat exchange between the external sources with the refrigeration cycle are estimated by using Equations (17) and (18) in the same conditions, respectively.

By replacing Equations (16) and (20) in Equation (19), it gives the following [30]:

$$COP_{endo}^{3T} = \frac{\dot{Q}_c}{\dot{Q}_h} = \left(\frac{T_c - \Delta T_2}{T_h - \Delta T_1}\right)\left(\frac{(T_h - \Delta T_1) - (T_{amb} + \Delta T_0)}{(T_{amb} + \Delta T_0) - (T_c - \Delta T_2)}\right) \tag{21}$$

The cold produced by such a tri-thermal machine can be used in several ways. It can be used for air conditioning of a building, or to meet a specific demand, such as the cooling of electronic devices like inverters. The final energy outputs of such a system are thus electricity and cold, which has to be optimized depending on the targeted application.

2.2.3. Active Cooling of an Additional PV Panel by an Endoreversible Tri-Thermal Machine

Another application of the cold produced by the tri-thermal machine is to provide an active cooling of an additional PV panel area to improve the overall electrical production. The impact of the active cooling PV panel by the endoreversible tri-thermal machine is therefore investigated here. As shown in Figure 5, the first panel (hot source) is maintained

at a first operating temperature T_h, while the second panel is cooled and maintained at a second operating temperature T_c (cold source) by the endoreversible tri-thermal machine. As the amount of cold produced $\dot{Q}_c$ is fixed by these operating temperatures, then a given surface S_2 of the second PV panel can be maintained at that temperature T_c.

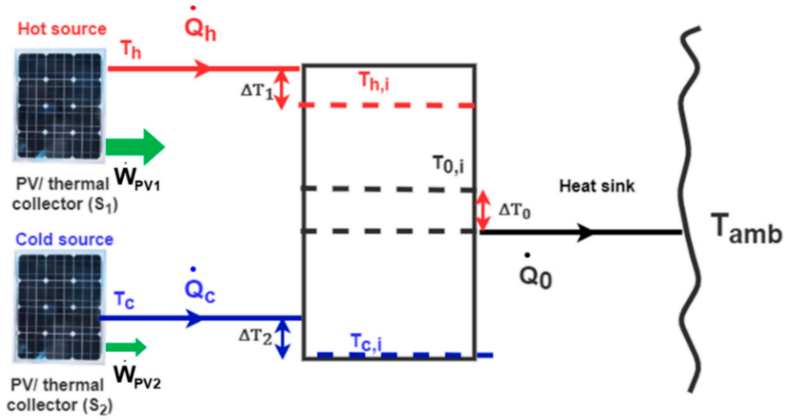

Figure 5. Cooling a second PV panel by an endoreversible tri-thermal machine coupled to a PV/TC system.

The working conditions of the second panel at this temperature allow for a better electrical efficiency as it is maintained at a temperature lower than the ambient one or at least at the ambient temperature. Thus, for this coupling configuration, the only energy output of the system is the electrical work. The performance of both PV panels must be optimized so as to reach the maximum global electrical performance. The thermal energy at T_h produced by a surface S_1 of the first PV panel is used as the driving heat source of the tri-thermal machine. The cold produced at temperature T_c maintains the second PV panel surface S_2 at this temperature. Thus, depending on the cold temperature T_c, the surface S_2 is determined by the following set of relations characterizing the cooling performances of the system coupling the two PV panels with the endoreversible machine:

$$COP^{3T}_{endo} = \frac{\dot{Q}_c}{\dot{Q}_h} = \frac{S_2\left[I_{rr} - \dot{Q}_{conv}(T_c) - \dot{Q}_{rad}(T_c) - \dot{W}_{PV2}(T_c)\right]}{S_1\left[I_{rr} - \dot{Q}_{conv}(T_h) - \dot{Q}_{rad}(T_h) - \dot{W}_{PV1}(T_h)\right]} \tag{22}$$

$$COP^{3T}_{endo} = \frac{\dot{Q}_c}{\dot{Q}_h} = \frac{(US)_c \Delta T_2}{(US)_h \Delta T_1} \tag{23}$$

where Equation (23) can be developed and written as Equation (21).

The electricity produced by these two panels of surface S_1 and S_2 is then compared to the production of the same surface of purely PV panel (S_1 + S_2) under the same conditions, but without being cooled or recovering heat (i.e., operating at stagnation temperature T_{st}). The overall electrical gain is defined as:

$$Gain_{PV1+PV2} = \frac{\left(\dot{W}_{PV1}(T_h)S_1 + \dot{W}_{PV2}(T_c)S_2\right) - \dot{W}_{PV}(T_{st})(S_1 + S_2)}{\dot{W}_{PV}(T_{st})(S_1 + S_2)} \tag{24}$$

This overall electrical gain can be compared to the electrical gain obtained for each PV panel that can also be defined as:

$$Gain_{PV1} = \frac{\dot{W}_{PV1}(T_h) - \dot{W}_{PV}(T_{st})}{\dot{W}_{PV}(T_{st})} \;\; and \;\; Gain_{PV2} = \frac{\dot{W}_{PV2}(T_c) - \dot{W}_{PV}(T_{st})}{\dot{W}_{PV}(T_{st})} \tag{25}$$

3. Results and Discussion

The results of the analyses described in this section are performed considering the actual characteristics of the PV panels manufactured by SUNPOWER (SPR-Max2-360-COM) and resumed in Table 1. The study is performed considering an ambient temperature of 40 °C, a wind speed of 1 m·s^{-1}, and several solar irradiations from 400 to 1000 W·m^{-2}. A simulation tool was developed in the Python environment to solve the equations of the thermodynamic model presented in the previous section.

Table 1. Main parameters considered for the performance evaluation of PV/TC.

Item	Value
Electrical efficiency at STC conditions η_{ref} (%)	20.4
Temperature coefficient β_{ref} (K^{-1})	0.0035
Effectiveness absorptivity $(\alpha\tau)$ (-)	0.95
Emissivity of glass ε (-)	0.9

3.1. Energy and Exergy Analysis of a PV/TC Panel Alone

Figure 6 shows the evolution of electrical and thermal powers generated by 1 m^2 of the chosen PV panel, as function of the operating temperature of the PV panel for different solar irradiations from 400 to 1000 W·m^{-2}. The PV panel temperature evolves from a maximum (or stagnation) temperature T_{st} varying from 81 °C to 40 °C. For this equilibrium temperature at a given solar irradiation, the electrical production is the lowest and no heat recovery is possible: all the generated heat is lost to the ambient environment. When heat is extracted from the PV panel, the temperature of the panel decreases, which increases the electrical energy produced and the thermal energy that can be recovered. This evolution is quasi-linear (even if the radiation losses evolution is not linear with the sky) for the global energy of the system. As expected, the best performances are achieved when the panel operating temperature is equal to the ambient one.

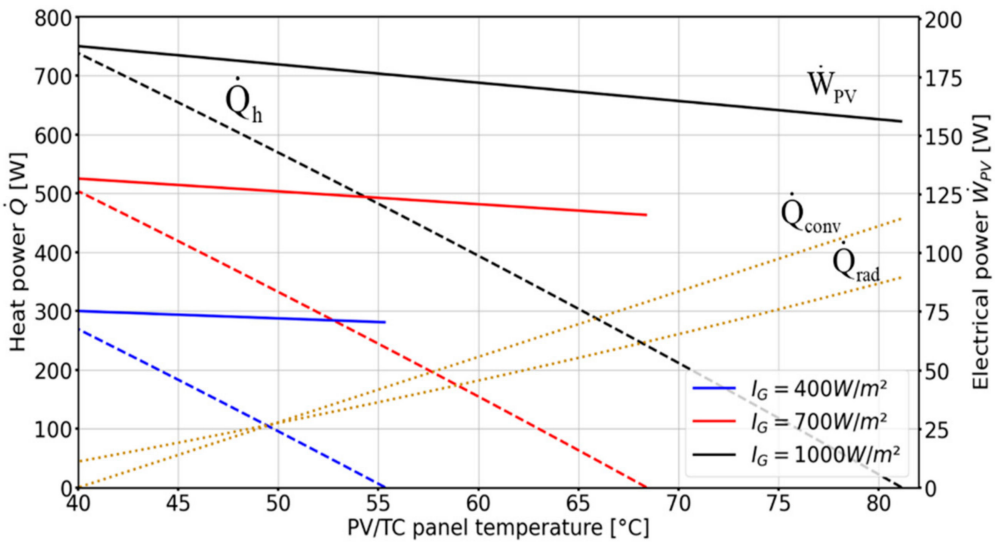

Figure 6. Variation of thermal ($\dot{Q}_h$ in blue, red and black dashed lines) and electrical power ($\dot{W}_{PV}$ in blue, red and black solid lines) of the PV/TC and losses ($\dot{Q}_{conv}$ and $\dot{Q}_{rad}$ in yellow dotted line) with its operating temperature for different solar irradiations.

Regarding the thermal energy generated from the PV/TC, if no heat is recovered when operating under a solar irradiation of 1000 W·m^{-2}, the panel will reach the thermal equilibrium with a maximal achievable temperature corresponding to an electrical production of 156 W·m^{-2} and 0 W·m^{-2} of thermal energy. The low temperature of the PV/TC panel allows us to reduce energy losses to reach, at ambient temperature, a maximum

electricity production of 188 W·m^{-2}, a maximum thermal energy production of 738 W·m^{-2}, and the convective heat losses to the environment that are null. The working temperature of the PV panel has a great importance; it has an impact on the utility of the recovered heat, as it can be seen in the exergy analysis that is carried out hereafter.

Figure 7 shows the evolution of the thermal, electrical, and overall exergy of the PV/TC panel operating under the same operating conditions as defined previously in the energy analysis. Contrarily to the linear evolution of the different forms of energy, only the electrical exergy evolves in a linear way with the cooling of the panel due to its definition as equivalent to the electrical energy. The thermal exergy increases from 0 W·m^2 when the PV/TC is at the stagnation temperature T_{st} to reach a maximum value of 25 W·m^{-2} for a solar radiation of 1000 W·m^{-2} and then decreases with the decrease of the PV panel temperature to again reach a null value when the PV panel operates at ambient temperature. As it can be noticed in Figure 7, for each solar irradiation, two optimum operating temperatures T_h^* and $\widetilde{T}_h$ can be defined as follows: the first one corresponds to the temperature that maximizes the overall exergy content, and the second one corresponds to the temperature that maximizes the thermal exergy content. The maximum exergy content of the thermal energy for solar radiation of 1000 W·m^{-2} is obtained when the PV panel operates at 62 °C, which corresponds from Figure 6 to a heat production of around 380 W·m^{-2} and an electrical production of 170 W·m^{-2}. Despite the high amount of heat recovered at the ambient temperature, the thermal exergy is null because the dead state (thermal equilibrium with the environment) is reached, as we can see in Equation (11). Regarding the evolution of the global exergy of the PV/TC, it increases as the PV panels cool. After the temperature of 62 °C for which the thermal exergy is maximum, the overall exergy continues to increase even though the thermal exergy degrades because the electrical exergy increases and compensates for this degradation. The overall exergy then reaches a maximum of 200 W·m^{-2} for a PV operating temperature of 54 °C and slightly decreases to equal the electrical exergy obtained by the PV panel when operating at an ambient temperature. It can be noticed that the thermal exergy is much lower than the electrical exergy because of the low operating temperature of the collector.

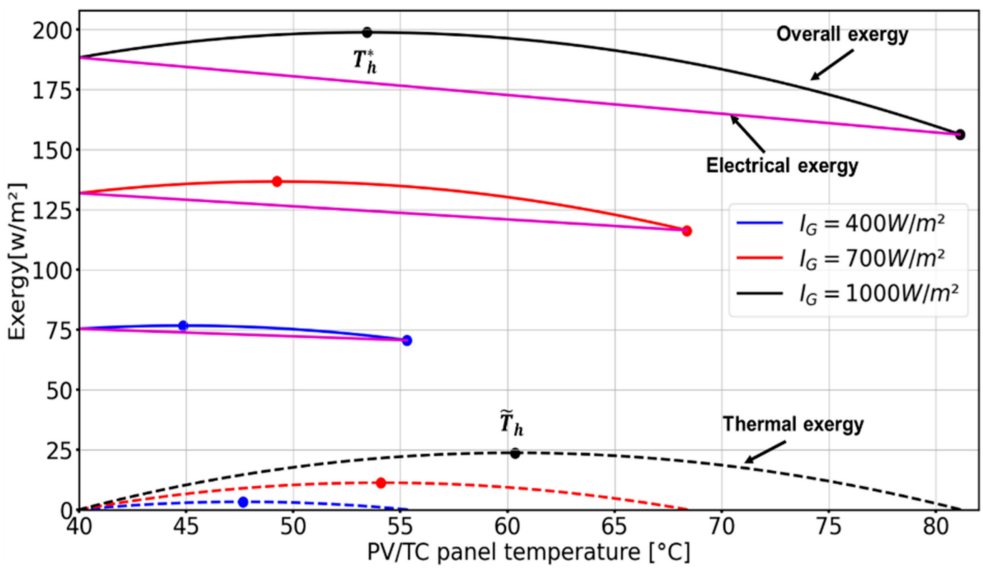

Figure 7. Variations of the PV/TC system of the thermal (blue, red and black dashed lines), electrical (purple solid lines), and overall exergies (blue, red and black solid lines) with its operating temperature for different solar irradiations. Optimal operating temperatures T_h^* and $\widetilde{T}_h$ are represented by dots.

The exergy amounts produced by the PV/TC panels depend on the incoming solar irradiation. When the solar irradiation decreases, the stagnation temperature also decreases as well as the optimal temperatures that maximize the thermal and overall produced exergy.

These optimal temperatures decrease almost linearly with decreasing solar irradiation as presented in Figure 8. The stagnation temperature varies between 81 °C and 46 °C with the variation of solar irradiation from 1000 W·m^{-2} to 200 W·m^{-2}. These values are similar to those obtained in the study carried out by Jakhrani et al. [31], who proposed several experimentally validated correlations for the evaluation of the stagnation temperature of a PV panel for various solar irradiations. Although the operating ambient conditions are not exactly identical, it can be noticed that the results presented in this work are close to those obtained by Jakhrani et al.

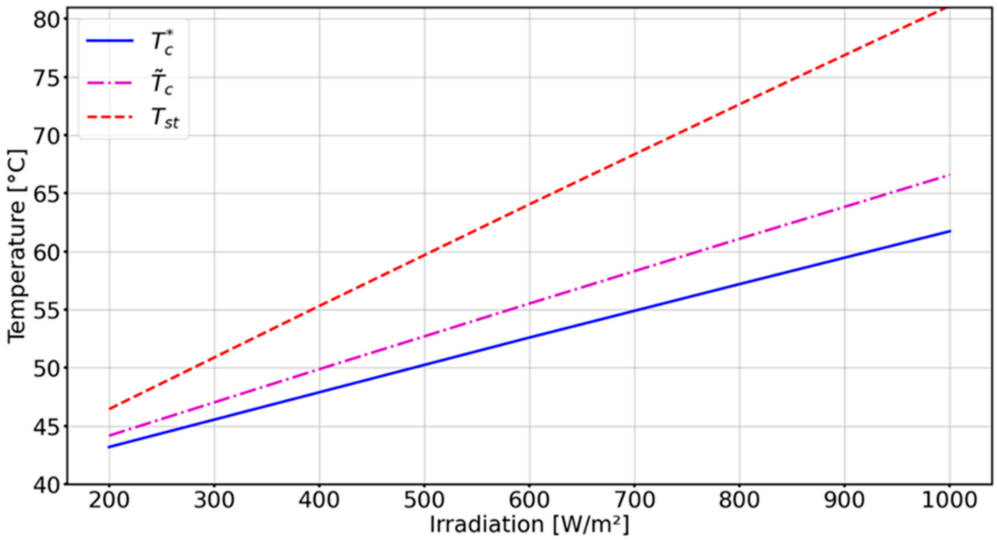

Figure 8. Variation of the equilibrium temperature T_{st}, and the optimal temperatures T_h^* and $\widetilde{T}_h$ with solar irradiation.

3.2. Performance Analysis of the Coupling of a PV/TC Panel with an Endoreversible Carnot Engine

Figure 9 presents the work that can be produced by an endoreversible engine cycle driven by a PV/thermal collector delivering heat at T_h. The temperature differences ΔT_0 and ΔT_1 are calculated using Equations (17) and (18) taking the values of global heat conductance as $(US)_0$ = 300 W·K^{-1} and $(US)_h$ = 50 W·K^{-1}. These values are taken for a realistic heat exchange coefficient where $(US)_0$ is considered larger than $(US)_h$, and therefore ΔT_0 is smaller than ΔT_1. One can see in Figure 9 that the produced work increases from zero to a maximum value and decreases after up to zero when the PV panel temperature decreases, while the temperature difference required for the heat exchange ΔT_1 between the PV panel and the engine cycle increases linearly. For a solar irradiation of 1000 W·m^{-2}, an optimum operating ΔT_1 for the heat exchange of about 5.5 °C enables to produce a maximum work of 16.5 W·m^{-2}, corresponding to an optimum operating temperature of $\widetilde{T}_h$ = 68 °C for the PV panel. Note that the endoreversible engine cycle considered in this study is a simplified model of any engine. A similar approach has been considered by Fudholi et al., who experimentally studied the coupling between a PVT panels and a TEG module, which is a thermoelectric di-thermal generator [22]. For a solar irradiation of 1000 W·m^{-2}, the additional electricity production by the TEG module is about 12 W, which is of the same order of magnitude as the production of the endoreversible di-thermal engine considered here.

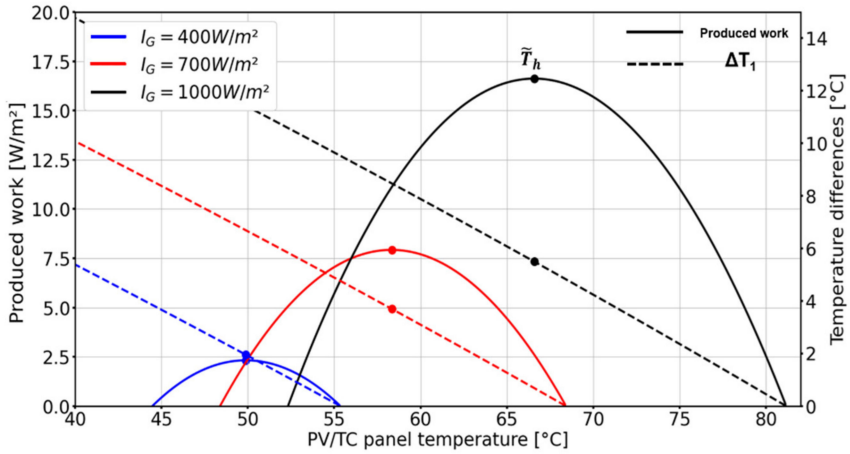

Figure 9. Variation of the work produced by the PV/TC system coupled to an endoreversible engine with its operating temperature and for different solar irradiations (black, red and blue solid curves). Variation of the corresponding heat exchange temperature difference ΔT_h required between the PV panel and the endoreversible engine cycle (black, red and blue dashed straight lines).

By considering the electricity and work production, the corresponding exergy efficiency of the global system is assessed and represented in Figure 10. For the electrical exergy efficiency, the evolution is similar to the electrical power evolution (Figure 6) as electrical energy is considered as full exergy: it starts at 15.5% for the maximum operating temperature of the PV panel of 81 °C (stagnation temperature under a solar irradiation of 1000 W·m^{-2}) and increases slightly as the PV panel is cooled down. The thermal exergy efficiency follows the same evolution as the work produced by the endoreversible engine: it starts at 0 for the PV panel's stagnation temperature, reaches a maximum value of 1.67% at $\widetilde{T}_h$, and decreases to zero as the PV panel's temperature decreases. As a result, the global exergy efficiency increases when the PV panel's temperature decreases, thanks firstly to the improvement of the electricity production and secondly to the valorization of the increasing amount of heat recovered from the PV panel by the endoreversible engine. This endoreversible cycle exploits this recovered heat produced to convert it into additional work: it reaches a maximum overall efficiency of about 18.7% for an optimal operating temperature of T_h^* = 62 °C under 1000 W·m^{-2} of solar irradiation. However, when the temperature of the PV panel decreases below this optimal operating temperature T_h^*, even if the electrical production increases slightly, the overall exergy efficiency decreases because of a significant decreasing of the work produced by the endoreversible engine.

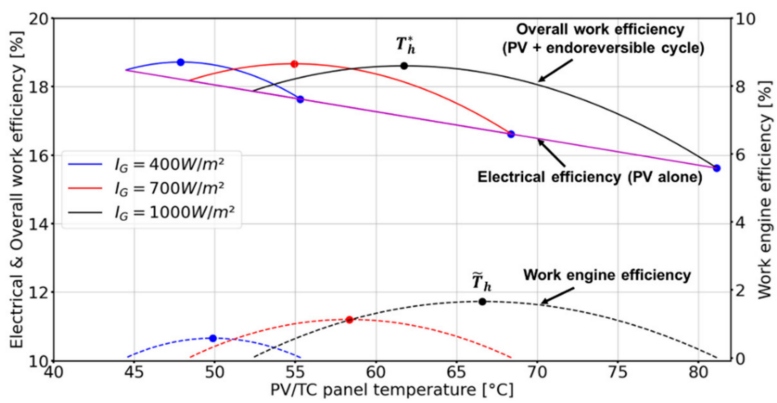

Figure 10. Variation of the PV/TC system coupled to an endoreversible engine of the work engine efficiency (blue, red and black dashed lines), electrical efficiency (purple solid lines), and overall efficiency (blue, red and black solid lines) as a function of the operating temperature of the PV panel.

Finally, by exploiting the thermal energy recovered from the PV panel to produce additional work through an endoreversible Carnot machine, it should be possible to achieve higher overall performances by further converting the produced work into additional electricity. The overall electrical performance obtained by such coupling should be close and higher than to those obtained by a conventional PV panel operating at ambient temperature, whatever the solar irradiation. The electricity produced by this PV panel operating at STC conditions (ambient conditions at 25 °C under 1000 W·m^{-2}) is about 188 W·m^{-2}, while the overall exergy achieved by this PV panel operating at $\widetilde{T}_h$ = 62 °C coupled to the endoreversible engine is about 186 W·m^{-2}.

3.3. Performance Analysis of the Coupling of a PV/TC Panel with a Tri-Thermal Endoreversible Machine for Cold Production

For each amount of thermal energy recovered from the PV panel at a temperature T_h, a resulting amount of cold is produced, which also depends on the desired cold temperature T_c. It can be seen from Equation (21) that the lower the temperature reached in the cold production, the less is the quantity of produced cold. Figure 11 represents the evolution of the produced cold by such a tri-thermal machine as a function of the desired cold temperature when coupled to 1 m^2 of panel delivering heat $\dot{Q}_h$ at the previously defined optimal operating PV panel temperatures, $\widetilde{T}_h$ and T_h^*.

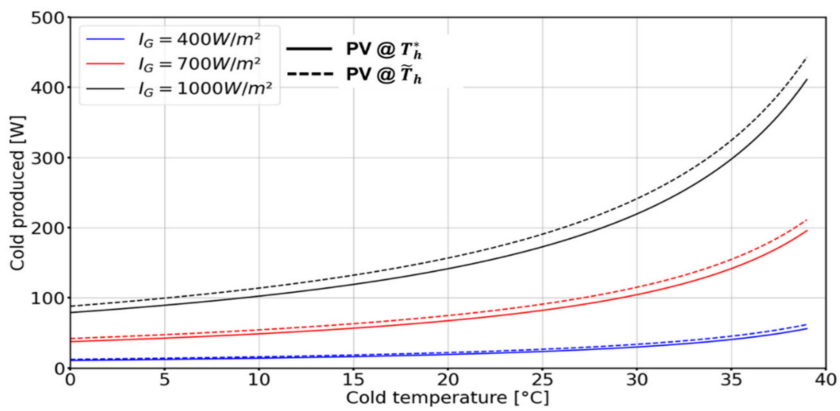

Figure 11. Cold produced at different temperature *Tc* by an endoreversible tri-thermal machine coupled to the PV/TC system working at $\widetilde{T}_h$ (blue, red and black dashed lines) and at T_h^* (blue, red and black solid lines).

The produced cold corresponds to that delivered in the optimum operating conditions of a hot PV panel that maximizes either its overall exergy (T_h^*) or just its thermal exergy ($\widetilde{T}_h$), as seen previously in Figure 10. For 288 W·m^{-2} of thermal energy delivered by the PV panel at $\widetilde{T}_h$ = 68 °C (Figure 6), 143 W·m^{-2} of cold at 20 °C can be produced under a solar irradiation of 1000 W·m^{-2}, while only 128 W·m^{-2} of cold can be produced at 20 °C when the PV panel operates at the optimum temperature T_h^* = 62 °C, which maximizes the overall exergy production of the panel with 380 W·m^{-2} of recovered thermal energy. As seen previously in the coupled PV/TC system to a di-thermal endoreversible Carnot engine in Section 2.2.1, the amount of cold produced by the tri-thermal machine obtained at the temperature $\widetilde{T}_h$ corresponding to the maximum thermal exergy production by the PV panel is more important than the cold produced at T_h^*. Moreover, for a cold production at 20 °C, the coefficient of performance of the endoreversible tri-thermal machine is about 0.24 when operated with heat provided at $\widetilde{T}_h$ = 68 °C, while it is 0.21 when operated at T_h^* = 62 °C. The cooling performances of these tri-thermal endoreversible machines that are considered in this study are closed and similar to those obtained by the silica gel/water adsorption cycle operating in the same temperature range [32].

3.4. Electrical Performance Enhancement Provided by an Active Cooling of Additional PV Panel by the Endoreversible Tri-Thermal Machine

The evolution of these electrical gains is represented in the Figure 12 as a function of the cooled PV temperature, as well for different solar irradiations.

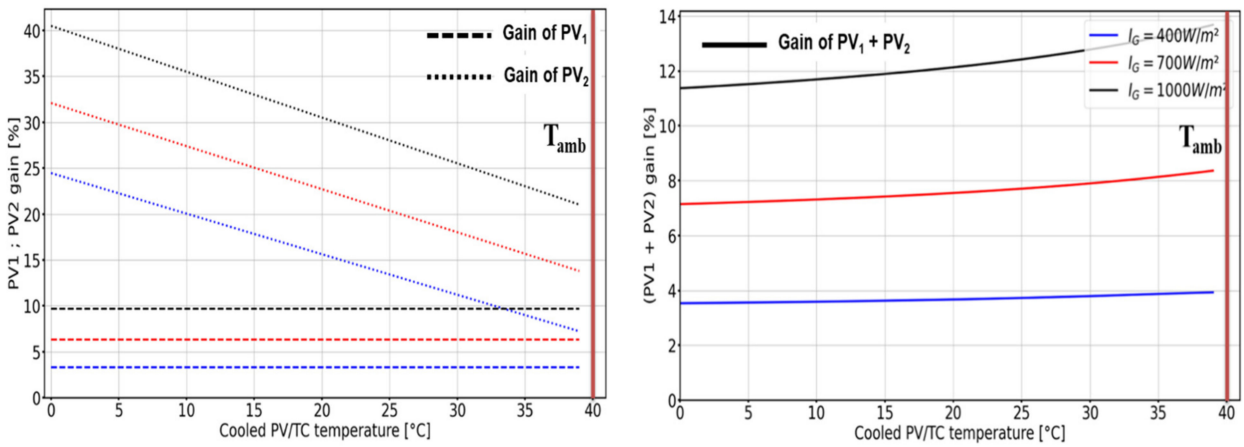

(**a**) (**b**)

Figure 12. (**a**) Variation for different solar irradiations of the electrical gains of both panels PV_1 (blue, red and black dashed lines) and PV_2 (blue, red and black doted lines) with the cooled PV_2 temperature T_c when PV_1 panel operates at its optimal temperature T_h^*. (**b**) Overall electricity production gain (blue, red and black solid lines).

Figure 12 shows that the gain of the first PV_1 panel working at the optimal global exergy temperature T_h^* is not impacted by the operating temperature of the second PV_2 panel *Tc*. Its gain is constant as its operating temperature is kept fixed and depends only on the solar irradiation: the gain is about 9.84% for a solar irradiation of 1000 $W \cdot m^{-2}$ and an ambient temperature of 40 °C. For the second panel that is actively cooled below the ambient temperature, it can be noticed that the lower the temperature is, the more important the gain is with a linear evolution that can reach 40% of gain for these operating conditions.

The overall electricity production gain increases slightly when the operating temperature T_c of the cooled panel is close to the ambient temperature, because in such a temperature range, the amount of cold produced by the tri-thermal machine increases from 80 $W \cdot m^{-2}$ to 430 $W \cdot m^{-2}$ and allows us to maintain a larger surface S_2 at T_c. The electrical production of the second panel becomes more substantial and makes the overall gain increase to reach 12.81% when the second PV panel is at temperature T_c = 30 °C.

3.5. Comparison with Conventional Cooling System by Heat Dissipation

Figure 13 shows a comparison of the performances of this active cooling of PV panels performed by a tri-thermal machine with a simple heat dissipation system of PV panels to ambient temperature, such as a water-cooled heat exchanger or a phase change material placed on the back side of the PV panel. Such a heat dissipation system conventionally enables the PV panels to operate generally from 15 to 25 °C above the ambient temperature.

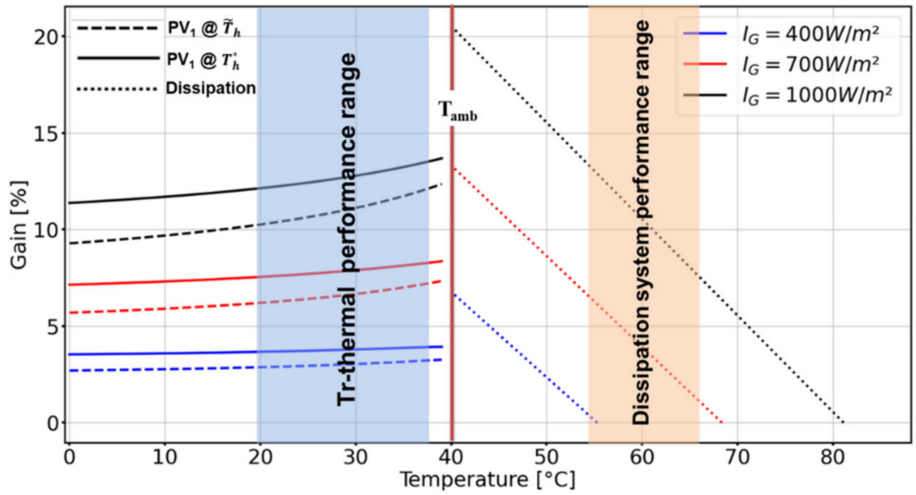

Figure 13. Electrical gains obtained with an ideal active cooling with a tri-thermal machine working at $\widetilde{T}_h$ (blue, red and black dashed lines) and at T_h^* (blue, red and black solid lines), and comparison with a heat dissipation system (blue, red and black doted lines).

When operating with an endoreversible tri-thermal refrigeration machine, the overall electrical performance is a bit higher than the one obtained by a heat dissipation device, such as a heat exchanger on the back side of the PV panel. Heat dissipation systems keep PV panels at least at T_{amb} + 15 °C, with water forced convection or phase change materials. To make a fair comparison between the tri-thermal active cooling with the heat dissipation systems, a reference case in terms of operating conditions is considered at this temperature of T_{amb} + 15 °C, where the two systems meet the same performance. One can notice that the tri-thermal machine allows for more flexibility in terms of gains achieved in comparison with the heat dissipation system. For these operating conditions, for the same surface of panel, the electrical gain achieved by the heat dissipation system keeping the PV panel at a temperature (T_{amb} + 15 °C) is equal to or lower than the gain obtained when the tri-thermal machine operates at T_h^*, whatever the temperature T_c of the cold produced. Unlike the heat dissipation system, to ensure this gain, the operating parameters of the panels temperature must be set at $T_h = T_{amb}$ + 12/15 °C or lower. Finally, it can be noticed in Figure 13 that the gains obtained in the T_h^* operating conditions are higher than the gains obtained in the $\widetilde{T}_h$ operating conditions. This is because, even though the amount of cooling is higher at $\widetilde{T}_h$ operating conditions and maintains a larger S_2 area of PV_2 at T_c, operating conditions at T_h^* have a higher gain than $\widetilde{T}_h$ for the same S_1 area.

4. Conclusions

The objective of this study was to investigate the potential operating conditions to improve the overall efficiency of a PV panel induced by the recovery of the thermal energy produced by the latter and its possible valorization into work or cold.

A thermodynamic analysis of the coupling of PV panels with an endoreversible Carnot engine was presented and showed that there are two optimal panel operating temperatures $\widetilde{T}_h$ and T_h^*, respectively, which allow us to maximize the thermal exergy produced by the PV panel, and thus its potential to be valorized into work (or electricity) or to maximize the overall thermal and electrical exergy of the PV panel.

The analysis of the valorization of the recovered heat into cold by an endoreversible tri-thermal machine showed that the amount of cold produced is higher if the PV panel operates at temperature $\widetilde{T}_h$ than at T_h^*. This difference is related to the higher thermal exergy content available at $\widetilde{T}_h$ than T_h^*. As a result, the coefficient of performance of this endoreversible tri-thermal machine is 0.24 when using PV heat at $\widetilde{T}_h$ and 0.21 for T_h^* operating conditions.

In the case of an active cooling of an additional PV panel surface, the electrical gains obtained for these two optimum temperatures of operation increase jointly when the produced cold temperature is close to the ambient temperature. However, operation at the optimum temperature T_h^* ensures a more stable gain when the operating temperature of the second cooled panel varies, with a slightly larger gain for the low temperatures of the cooled panel of about 12.8% in comparison with the working conditions at $\widetilde{T}_h$ of about 11.1% at T_c = 30 °C and 1000 W·m^{-2}.

By comparing the performances of the active cooling system with conventional heat dissipative systems identified as state of the art, it is found that the endoreversible tri-thermal machine enables us to reach similar performances when the cooled PV temperature T_c is at 20 °C, as dissipative systems enable the PV panel to work at T_{amb} + 15 °C. Accordingly, this active cooling solution can be considered as technically competitive with the heat dissipative systems based on forced water convection or heat pipe.

Coupling such a tri-thermal machine with PV panels could be relevant to prevent the deterioration of the PV panel over time, thanks to a lower average operating temperature. The conclusions of this theoretical study must be confirmed by a transient behavior analysis of the PV/Thermal collector panel and an experimental approach.

Author Contributions: Conceptualization, A.I., D.S., M.P.-M. and D.A.-P.; methodology, D.S., M.P.-M. and D.A.-P.; software, A.I.; validation, D.S., M.P.-M. and D.A.-P.; formal analysis, A.I.; data curation, A.I. and D.A.-P.; writing—original draft preparation, A.I.; writing—review and editing, A.I., D.S., M.P.-M. and D.A.-P.; supervision, D.S., M.P.-M. and D.A.-P.; project administration, D.S.; funding acquisition, D.S. and D.A.-P. All authors have read and agreed to the published version of the manuscript.

Funding: This research was funded by TotalEnergies and the National French Association of Research and Technology.

Institutional Review Board Statement: Not applicable.

Informed Consent Statement: Not applicable.

Data Availability Statement: Not applicable.

Acknowledgments: The authors would like to thank the company TotalEnergies (France) and the National French Association of Research and Technology (ANRT-CIFRE) for funding and supporting this research work.

Conflicts of Interest: The authors declare no conflict of interest.

Nomenclature

C	Heat capacity of the collector (J·kg ^{1}·K^{-1})
COP	Coefficient of performance
$\dot{E}x$	Exergy per unit area of collector (W·m^{-2})
h	Convective heat transfer coefficient (W·m^{-2} K^{-1})
I_G	Global incident irradiation (W·m^{-2})
m	Mass (kg)
PCM	Phase change material
PV	Photovoltaic panel
PVT	Photovoltaic-thermal panel
$\dot{Q}$	Thermal power per unit area of collector (W·m^{-2})
S	Area (m^2)
STC	Standard test conditions
T	Temperature (K)
TEG	Thermoelectric generator module
TREC	Thermally regenerative electrochemical cycle
V	Wind velocity (m·s^{-1})
$\dot{W}$	Electrical power per unit area of collector (W·m^{-2})

Greek symbol	
α	Absorptivity
β	Temperature coefficient of PV module efficiency (K^{-1})
ε	Emissivity
η	Efficiency
σ	Stefan–Boltzmann constant ($W \cdot m^{-2} \cdot K^{-4}$)
τ	Transitivity
Indices	
amb	Ambient
c	Carnot, Cold.
conv	Convective
des	Destroyed
PV	Photovoltaic panel
endo	Endoreversible
ex	Exergie
h	Heat
G	Global incident
gl	Overall
rad	Radiative
ref	Reference
s	Solar
sky	Sky
st	Stagnation
t	Time
th	Thermal
w	Wind

References

1. Koebrich, S. *Renewable Energy Data Book*; United States Department of Energy: Washington, DC, USA, 2018; p. 149. Available online: https://www.nrel.gov/docs/fy20osti/75284.pdf (accessed on 1 December 2021).
2. Shockley, W.; Queisser, H.J. Detailed Balance Limit of Efficiency of *p-n* Junction Solar Cells. *J. Appl. Phys.* **1961**, *32*, 510–519. [CrossRef]
3. Li, H.; Zhao, J.; Li, M.; Deng, S.; An, Q.; Wang, F. Performance analysis of passive cooling for photovoltaic modules and estimation of energy-saving potential. *Sol. Energy* **2019**, *181*, 70–82. [CrossRef]
4. Cuce, E.; Cuce, P.M.; Karakas, I.H.; Bali, T. An accurate model for photovoltaic (PV) modules to determine electrical characteristics and thermodynamic performance parameters. *Energy Convers. Manag.* **2017**, *146*, 205–216. [CrossRef]
5. Skoplaki, E.; Palyvos, J.A. On the temperature dependence of photovoltaic module electrical performance: A review of efficiency/power correlations. *Sol. Energy* **2009**, *83*, 614–624. [CrossRef]
6. Nehme, B.; M'Sirdi, N.K.; Akiki, T.; Naamane, A.; Zeghondy, B. Photovoltaic panels life span increase by control. In *Predictive Modelling for Energy Management and Power Systems Engineering*; Elsevier: Amsterdam, The Netherlands, 2021; pp. 27–62. ISBN 978-0-12-817772-3. [CrossRef]
7. Ogbomo, O.O.; Amalu, E.H.; Ekere, N.N.; Olagbegi, P.O. Effect of operating temperature on degradation of solder joints in crystalline silicon photovoltaic modules for improved reliability in hot climates. *Sol. Energy* **2018**, *170*, 682–693. [CrossRef]
8. Sathe, T.M.; Dhoble, A.S. A review on recent advancements in photovoltaic thermal techniques. *Renew. Sustain. Energy Rev.* **2017**, *76*, 645–672. [CrossRef]
9. Bahaidarah, H.M.; Baloch, A.A.; Gandhidasan, P. Uniform cooling of photovoltaic panels: A review. *Renew. Sustain. Energy Rev.* **2016**, *57*, 1520–1544. [CrossRef]
10. Du, D.; Darkwa, J.; Kokogiannakis, G. Thermal management systems for Photovoltaics (PV) installations: A critical review. *Sol. Energy* **2013**, *97*, 238–254. [CrossRef]
11. Chow, T.T. A review on photovoltaic/thermal hybrid solar technology. *Appl. Energy* **2010**, *87*, 365–379. [CrossRef]
12. Bjørk, R.; Nielsen, K.K. The maximum theoretical performance of unconcentrated solar photovoltaic and thermoelectric generator systems. *Energy Convers. Manag.* **2018**, *156*, 264–268. [CrossRef]
13. Fathabadi, H. Two novel methods for converting the waste heat of PV modules caused by temperature rise into electric power. *Renew. Energy* **2019**, *142*, 543–551. [CrossRef]
14. Chow, T.T.; Pei, G.; Fong, K.F.; Lin, Z.; Chan, A.L.S.; Ji, J. Energy and exergy analysis of photovoltaic–thermal collector with and without glass cover. *Appl. Energy* **2009**, *86*, 310–316. [CrossRef]
15. Bandaru, S.H.; Becerra, V.; Khanna, S.; Radulovic, J.; Hutchinson, D.; Khusainov, R. A Review of Photovoltaic Thermal (PVT) Technology for Residential Applications: Performance Indicators, Progress, and Opportunities. *Energies* **2021**, *14*, 3853. [CrossRef]

16. Sarafraz, M.M.; Safaei, M.R.; Leon, A.S.; Tlili, I.; Alkanhal, T.A.; Tian, Z.; Goodarzi, M.; Arjomandi, M. Experimental Investigation on Thermal Performance of a PV/T-PCM (Photovoltaic/Thermal) System Cooling with a PCM and Nanofluid. *Energies* **2019**, *12*, 2572. [CrossRef]
17. Zhou, C.; Liang, R.; Riaz, A.; Zhang, J.; Chen, J. Experimental investigation on the tri-generation performance of roll-bond photovoltaic thermal heat pump system during summer. *Energy Convers. Manag.* **2019**, *184*, 91–106. [CrossRef]
18. Zhou, J.; Ma, X.; Zhao, X.; Yuan, Y.; Yu, M.; Li, J. Numerical simulation and experimental validation of a micro-channel PV/T modules based direct-expansion solar heat pump system. *Renew. Energy* **2020**, *145*, 1992–2004. [CrossRef]
19. Poredoš, P.; Tomc, U.; Petelin, N.; Vidrih, B.; Flisar, U.; Kitanovski, A. Numerical and experimental investigation of the energy and exergy performance of solar thermal, photovoltaic and photovoltaic-thermal modules based on roll-bond heat exchangers. *Energy Convers. Manag.* **2020**, *210*, 112674. [CrossRef]
20. Obalanlege, M.A.; Mahmoudi, Y.; Douglas, R.; Ebrahimnia-Bajestan, E.; Davidson, J.; Bailie, D. Performance assessment of a hybrid photovoltaic-thermal and heat pump system for solar heating and electricity. *Renew. Energy* **2020**, *148*, 558–572. [CrossRef]
21. Bombarda, P.; Di Marcoberardino, G.; Lucchini, A.; Leva, S.; Manzolini, G.; Molinaroli, L.; Pedranzini, F.; Simonetti, R. Thermal and electric performances of roll-bond flat plate applied to conventional PV modules for heat recovery. *Appl. Therm. Eng.* **2016**, *105*, 304–313. [CrossRef]
22. Fudholi, A.; Sopian, K.; Yazdi, M.H.; Ruslan, M.H.; Ibrahim, A.; Kazem, H.A. Performance analysis of photovoltaic thermal (PVT) water collectors. *Energy Convers. Manag.* **2014**, *78*, 641–651. [CrossRef]
23. Joshi, A.S.; Tiwari, A. Energy and exergy efficiencies of a hybrid photovoltaic–thermal (PV/T) air collector. *Renew. Energy* **2007**, *32*, 2223–2241. [CrossRef]
24. Sobhnamayan, F.; Sarhaddi, F.; Alavi, M.A.; Farahat, S.; Yazdanpanahi, J. Optimization of a solar photovoltaic thermal (PV/T) water collector based on exergy concept. *Renew. Energy* **2014**, *68*, 356–365. [CrossRef]
25. Evans, D.L. Simplified method for predicting photovoltaic array output. *Sol. Energy* **1981**, *27*, 555–560. [CrossRef]
26. Sharples, S.; Charlesworth, P.S. Full-scale measurements of wind-induced convective heat transfer from a roof-mounted flat plate solar collector. *Sol. Energy* **1998**, *62*, 69–77. [CrossRef]
27. Jones, A.D.; Underwood, C.P. A thermal model for photovoltaic systems. *Sol. Energy* **2001**, *70*, 349–359. [CrossRef]
28. Jeter, S.M. Maximum conversion efficiency for the utilization of direct solar radiation. *Sol. Energy* **1981**, *26*, 231–236. [CrossRef]
29. Haseli, Y. Endoreversible heat engines. In *Entropy Analysis in Thermal Engineering Systems*; Academic Press: Mt Pleasant, MI, USA; Elsevier: London, UK, 2020; pp. 67–83. [CrossRef]
30. Meunier, F.; Neveu, P. Convertisseurs Thermiques—Machines Frigorifiques. Pompes à Chaleur. Thermotransformateurs. In Techniques de L'ingénieur Production de Froid Mécanique, Editions T.I., Ed.; Saint Denis, France 2018; p. 22. Available online: https://www.techniques-ingenieur.fr/base-documentaire/energies-th4/production-de-froid-mecanique-42211210/convertisseurs-thermiques-be9734/ (accessed on 1 December 2021). [CrossRef]
31. Jakhrani, A.Q.; Othman, A.K.; Rigit, A.R.H.; Samo, S.R. Comparison of Solar Photovoltaic Module Temperature Models. In Proceedings of the 2011 IEEE Conference on Clean Energy and Technology (CET), Kuala Lumpur, Malaysia, 27–29 June 2011; p. 8.
32. Cot-Gores, J.; Castell, A.; Cabeza, L.F. Thermochemical energy storage and conversion: A-state-of-the-art review of the experimental research under practical conditions. *Renew. Sustain. Energy Rev.* **2012**, *16*, 5207–5224. [CrossRef]